Journal of Bioenergetics and Biomembranes, Vol. 33, No. 3, 2001

Exploring the Catalytic Core of Complex I by *Yarrowia lipolytica* Yeast Genetics[1]

Stefan Kerscher,[2] Noushin Kashani-Poor,[2] Klaus Zwicker,[2] Volker Zickermann,[2] and Ulrich Brandt[2,3]

We have developed *Yarrowia lipolytica* as a model system to study mitochondrial complex I that combines the application of fast and convenient yeast genetics with efficient structural and functional analysis of its very stable complex I isolated by his–tag affinity purification with high yield. Guided by a structural model based on homologies between complex I and [NiFe] hydrogenases mutational analysis revealed that the 49 kDa subunit plays a central functional role in complex I. We propose that critical parts of the catalytic core of complex I have evolved from the hydrogen reactive site of [NiFe] hydrogenases and that iron–sulfur cluster N2 resides at the interface between the 49 kDa and PSST subunits. These findings are in full agreement with the "semiquinone switch" mechanism according to which coupling of electron and proton transfer in complex I is achieved by a single integrated pump comprising cluster N2, the binding site for substrate ubiquinone, and a tightly bound quinone or quinoid group.

KEY WORDS: Complex I, NADH:ubiquinone oxidoreductase; hydrogenase; yeast; *Yarrowia lipolytica*; mitochondria; ubiquinone; proton translocation.

INTRODUCTION

Exploring the catalytic core of respiratory chain complex I (NADH:ubiquinone oxidoreductase, EC 1.6.99.3) seems a formidable task, because of the enormous size and complexity of the enzyme: Mammalian complex I has a M_r of almost 1000 kDa and consists of 43 different subunits, seven of which are encoded by the mitochondrial genome (Walker, 1992; Skehel *et al.*, 1998). The application of time-resolved optical spectroscopy is hampered by the lack of chromophores characteristically absorbing in the visible range, like the heme groups in the cytochrome bc_1 complex or in cytochrome *c* oxidase. Yet, in recent years, there has been a constant rise of interest in complex I research, mainly sparked by its physiological and medical importance.

Complex I links electron transfer from NADH to ubiquinone to the pumping of four protons per two electrons (Wikström, 1984) across the inner mitochondrial or bacterial plasma membrane. This accounts for about 40% of the transmembrane proton gradient generated in NADH oxidation by the mitochondrial respiratory chain. Complex I is a prime source of reactive oxygen species generated within the mitochondrial matrix (Robinson, 1998) as its reaction mechanism includes the formation of semiquinone radical intermediates. Consequently, hereditary and acquired defects in complex I have been implicated in a large number of neurodegenerative disorders (Schapira, 1998) and even seem to promote aging (Wallace, 1999). While the role of mtDNA mutations as a major contributor to complex I deficiency (MIM 252010) has been widely recognized (Wallace, 1994, 1999), recent findings have shown that mutations in nuclear-coded subunits of complex I are also fairly common among the group of congenital OXPHOS defects and may result in diverse pathologies (Smeitink and Van den Heuvel, 1999; Schon, 2000). Among patients with isolated

[1] Key to abbreviations: DBQ, *n*-decylubiquinone; DQA, 2-decyl-4-quinazolinyl amine; EPR, electron paramagnetic resonance; HAR, hexamine-ruthenium(III)-chloride.

[2] Universitätsklinikum Frankfurt, Institut für Biochemie I, Zentrum der Biologischen Chemie, Theodor-Stern-Kai 7, Haus 25 B, D-60590 Frankfurt am Main, Germany.

[3] To whom all correspondence should be addressed. e-mail: brandt@zbc.klinik.uni-frankfurt.de

0145-479X/01/0600-0187$19.50/0

complex I deficiency, Leigh syndrome or subacute necrotizing encephalomyelopathy (MIM 25600) seems to be the most common clinical presentations (Robinson, 1998). Recently, it has been demonstrated that Leigh syndrome can be caused by point mutations in the nuclear genes *NDUFS8* (Loeffen *et al.*, 1998) and *NDUFS7* (Triepels *et al.*, 1999).

Of the many subunits of mammalian complex I, fourteen have homologs in the subunits of prokaryotic complex I (Yagi *et al.*, 1998). This "minimal form" of complex I apparently carries out the same catalytic function, although it has been reported recently that complex I from *Escherichia coli* can pump sodium ions in addition to or instead of protons (Krebs *et al.*, 1999; Steuber *et al.*, 2000). Five of these fourteen subunits are also homologous to subunits of certain membrane-bound [NiFe] hydrogenases (see below).

COMPLEX I FROM *Yarrowia lipolytica*

An ideal model organism for exploring complex I should contain a stable, easily purified enzyme and should be amenable to straightforward genetic manipulation. Complex I from various bacterial sources, with the notable exception of the sodium-pumping enzyme from *E. coli* (Leif *et al.*, 1995; Spehr *et al.*, 1999) tends to dissociate during purification (Herter *et al.*, 1997). On the other hand, genetic manipulation of complex I from *Bos taurus* and *Neurospora crassa* is either impossible or rather difficult.

As complex I does not exist in baker's yeast, *Saccharomyces cerevisiae*, we have chosen the obligate aerobic yeast *Yarrowia lipolytica* as our model system: This organism offers virtually all of the advantages that have made yeast genetics so powerful, including a simple haplo/diplontic life cycle, two naturally stable mating types called A and B, a high frequency of homologous recombination, a small genome with few introns, and several genetic markers that allow for both positive and negative selection (Barth and Gaillardin, 1996, 1997). Because of its proficiency in the secretion of extracellular proteins, *Y. lipolytica* is also an attractive system for the expression of heterologous proteins for biotechnological use (Madzak *et al.*, 1999, 2000). Special virtues of *Y. lipolytica* are the availability of replicative single-copy plasmids bearing chromosomal ARS/CEN regions and the high biomass yield of up to 100 g/l (wet weight). As a strictly aerobic organism, *Y. lipolytica* has a constantly high content of mitochondria with constitutive expression of respiratory chain enzymes, even in the presence of deleterious mutations.

We have cloned and sequenced the seven nuclear genes *NUAM*, *NUBM*, *NUCM*, *NUGM*, *NUHM*, *NUIM*, and *NUKM* (accession numbers AJ249781, 249782, AJ249783, AJ249784, AJ250338, AJ250340, and AJ250339) encoding central, highly conserved subunits of complex I (Djafarzadeh *et al.*, 2000). As expected from their homology to subunits of complex I from *Bos taurus* and *E. coli*, these subunits contain the binding site for the FMN cofactor and the ligands of iron–sulfur clusters N1–N6 (Table I). Seven more genes for highly conserved subunits of complex I, called ND1–ND6 and ND4L, are encoded by the mitochondrial genome in higher eukcaryotes. Their primary structures were derived from the complete mitochondrial genomic sequence (Kerscher *et al.*, 2001).

Complex I from *Y. lipolytica* is very stable and allows straightforward purification by conventional methods (Djafarzadeh *et al.*, 2000). His-tag purification has been achieved by attaching a six histidine tag or a six histidine tag preceded by a six alanine linker to the C-terminus of the 30 kDa subunit (Kashani-Poor *et al.*, 2001). Affinity purification of his-tagged complex I, followed by gel filtration, resulted in very pure enzyme (>95% as judged by SDS–PAGE) with a total yield of 38% and a specific NADH: HAR activity of 64 μmol $\times$ min^{-1} $\times$ mg^{-1} protein, equivalent to a purification factor of at least 60. Upon reconstitution into asolectin vesicles, the enzyme regained the original activity of 6.7 μmol $\times$ min^{-1} $\times$ mg^{-1} for the more physiological NADH:DBQ electron transfer reaction (Kashani-Poor *et al.*, 2001).

Two-dimensional (2D) reconstructions of single particles negatively stained with uranyl acetate or shock frozen in aqueous ice (Djafarzadeh *et al.*, 2000) and three-dimensional (3D) reconstructions of single particles negatively stained with ammonium molybdate (Radermacher *et al.*, in preparation) revealed that complex I from *Y. lipolytica*, like the enzyme from *E. coli*, *N. crassa*, and *Bos taurus*, is L shaped, with a membrane arm and a peripheral arm in perpendicular arrangement. However, in contrast to bovine heart complex I (Grigorieff, 1998), we did not observe a thin stalk connecting these two arms, which may explain the superior stability of the *Y. lipolytica* enzyme.

EPR spectroscopy at liquid helium temperatures allows characterization of paramagnetic iron–sulfur clusters in complex I (Ohnishi, 1998). X-band (9.47 GHz) EPR spectroscopy of purified *Y. lipolytica* complex I reduced with NADH revealed signals of five different iron–sulfur clusters (Djafarzadeh *et al.*, 2000) (Fig. 1). These were designated N1, N2, N3, N4, and N5, according to increasing spin relaxation rates (Ohnishi, 1998).

Cluster N1 of *Y. lipolytica* complex I can be detected at higher temperatures (45 K) than the other clusters. It is of binuclear type [2Fe–2S] and shows a nearly axial

Table I. Characteristic Features of the Fourteen Central Subunits of *Yarrowia lipolytica* Complex I

Gene symbol	*Bos taurus* homolog	Amino acids of: Open reading frame	Amino acids of: Mature protein	M_r of mature apoprotein	Processing site[a]	Iron–sulfur cluster binding motifs	Prosthetic groups in *B. taurus* and *E. coli*[b]
NUAM	75 kDa	728	694	75,195	A<u>R</u>RL | AEIE	C-(x)$_{10}$-CxxC-(x)$_{13}$-C-(x)$_{35}$-	N1b
						HxxxCxxC-(x)$_5$-C-(x)$_{40}$-	N5
						CxxCxxC-(x)$_{44}$-CP[c]	N4
NUBM	51 kDa	488	470	51,657	S<u>R</u>GF | ATTQ	CxxCxxC-(x)$_{39}$-C	FMN, N3
NUCM	49 kDa	466	444	49,942	A<u>R</u>YM | ATTA		
NUGM	30 kDa	281	251	29,225	A<u>R</u>AA | EAAP		
NUHM	24 kDa	243				CxxxxC-(x)$_{35}$-CxxxC	N1a
NUIM	TYKY	229				CxxCxxCxxxCP-(x)$_{27}$-	N6a, N6b
						CxxCxxCxxxCP	
NUKM	PSST	210	183	20,425	T<u>R</u>AY | SAPA	C-(x)$_{63}$-C-(x)$_{29}$-CP	N2
ND1	ND1	341	341	38,345			
ND2	ND2	469	469	53,329			
ND3	ND3	128	128	14,470			
ND4	ND4	486	486	54,478			
ND4L	ND4L	89	89	9,810			
ND5	ND5	655	655	73,701			
ND6	ND6	184	184	20,626			

[a] A vertical line marks the start of the mature protein as determined by Edman degradation. The −3 arginine is underlined.
[b] N1a and N1b are binuclear clusters, N2, N3, N4, and N5 are tetranuclear clusters (Ohnishi, 1998). N6a and N6b are EPR-silent tetranuclear clusters in a ferredoxin like arrangement (Kintscher *et al.*, 2000).
[c] According to (Finel, 1998).

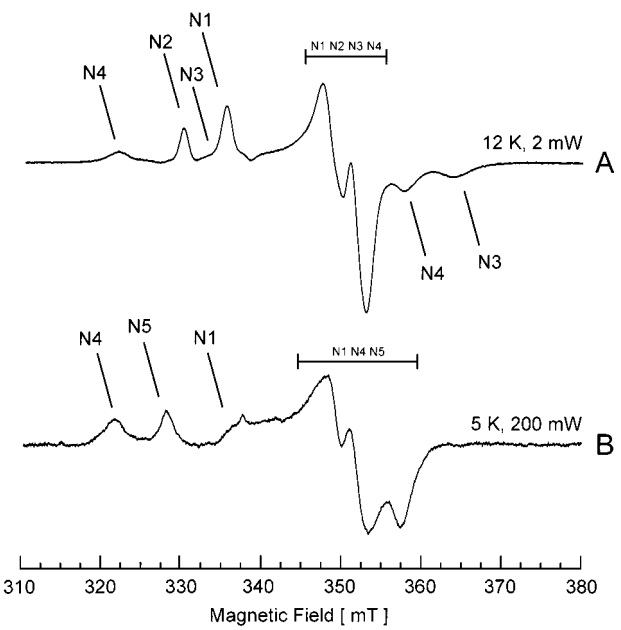

Fig. 1. EPR spectra of purified *Y. lipolytica* complex I reduced with NADH. (A) Contributions of four individual iron–sulfur clusters can be recognized in the spectrum at 12 K. Experimental conditions: microwave frequency, 9.47 GHz; modulation amplitude, 0.8 mT. (B) At temperatures below 10 K, a fifth iron–sulfur cluster (N5) can be detected. Under the conditions shown here, clusters N2, N3 are almost completely and cluster N1, N4 are largely power saturated. Experimental conditions: microwave frequency, 9.47 GHz, modulation amplitude 0.64 mT.

spectrum (not shown), meaning that only two different g values could be distinguished directly ($g_z = 2.02$, $g_{xy} = 1.94$). However, simulation of the spectrum revealed its rhombic character with three individual g values ($g_{z,y,x} = 2.018$, 1.945, and 1.933). Until now, we could not detect any additional binuclear clusters as reported for complex I from bovine heart mitochondria (N1a and N1b) (Ohnishi *et al.*, 1981) or *E. coli* (N1a, N1b, and N1c) (Sled *et al.*, 1993).

Because of their faster spin relaxation rates, all other clusters, which are of tetranuclear type, [4Fe–4S] were only detectable below 30 K. According to studies with purified bovine (Kowal *et al.*, 1986) and *N. crassa* complex I (Wang *et al.*, 1991), iron–sulfur cluster N2 ($g_{z,y,x} = 2.051$, 1.926, and 1.918) can be reduced selectively by sodium dithionite. The spectrum of cluster N2 also shows an almost axial line shape, but simulation revealed rhombic characteristics, as was the case with cluster N1. N2 has the slowest spin relaxation rates among the tetranuclear clusters, which allows detection of EPR spectra even at temperatures above 20 K.

Clusters N3 ($g_{z,y,x} = 2.031$, 1.930, and 1.861) and N4 ($g_{z,y,x} = 2.104$, 1.931, and 1.892) both show rhombic EPR spectra. At 5 K and high microwave power, N4 is still detectable, while N3 becomes almost completely saturated (Fig. 1B).

From comparison of an experimental spectrum of NADH-reduced enzyme recorded under nonsaturating conditions with simulated spectra of N1, N2, N3, and N4, a 1:1:1:1 stoichiometry was deduced for these four clusters.

At temperatures below 10 K and high microwave power, an additional iron–sulfur cluster, N5 ($g_{z,y,x}$ = 2.062, 1.93, and ~1.89), becomes detectable (Fig. 1B). Similar clusters could only be detected in complex I from bovine heart and *Rhodobacter sphaeroides* (Sled *et al.*, 1993). N5 of *Y. lipolytica* shows very fast spin relaxation with a half saturation parameter ($P_{1/2}$) of about 180 mW at 5 K. The spin concentration of this cluster is much lower than for the other clusters. However, spin concentration, meaning EPR-detectable concentration, does not necessarily reflect the stoichiometry of this cluster in the enzyme.

As commonly observed in ascomycetous fungi and in plants, the mitochondrial respiratory chain of *Y. lipolytica*, besides complex I, also contains a so called alternative NADH:ubiquinone oxidoreductase. These enzymes typically consist of a single polypeptide chain with a molecular weight of 50 to 60 kDa and contain one molecule of noncovalently bound FAD as redox prosthetic group. They catalyze the same redox reaction as complex I but do not translocate protons across the membrane. Different alternative NADH:ubiquinone oxidoreductases exhibit one fundamental variation: they may either reside on the outer or the inner face of the mitochondrial inner membrane. In the case of *S. cerevisiae*, one internal and two external alternative NADH:ubiquinone oxidoreductases (Luttik *et al.*, 1998) are present. *Y. lipolytica*, by contrast, has only one single, external enzyme called NDH2 (Kerscher *et al.*, 1999), a minimal configuration that may be reminiscent of the ancestral situation. External alternative NADH:ubiquinone oxidoreductase cannot complement for loss of function mutations affecting complex I. Recovery of deletion mutations in the genes for essential subunits of complex I has been achieved by targeting the NDH2 protein to the matrix side using the presequence of the NUAM (75 kDa) protein of *Y. lipolytica* complex I (Kerscher *et al.*, submitted). Cells harboring this NDH2i fusion gene, either on a replicative plasmid or randomly integrated into the genome display resistance to complex I inhibitors like DQA, which allows for convenient selection.

In summary, we have taken the following steps to generate *Y. lipolytica* strains for the functional analysis of complex I: (1) generation of deletions (marked with *URA3* or *LEU2*) in every single gene for the central, nuclear-coded subunits of complex I by double homologous recombination, (2) incorporation of the genes for the his-tagged 30 kDa subunit (by homologous recombination following the pop-in–pop-out strategy) and for NDH2i (by random integration) into the genome, and (3) introduction of site-directed mutations in genes deleted on the chromosome using replicative single-copy plasmids (marked with *URA3*, *LEU2*, or *HygB*^{R}).

THE CATALYTIC CORE OF COMPLEX I

Constraints from Functional Studies

Several mechanistic models for electron transfer and proton pumping by complex I have been proposed (Dutton *et al.*, 1998; Degli Esposti and Ghelli, 1994; Brandt, 1997). Because of the lack of experimental evidence and a molecular structure of complex I, all of them have to be considered as highly speculative. Constraints can be derived from the experimentally found proton-pumping stoichiometry of $2H^+/e^-$ (Wikström, 1984), the location and properties of the redox groups (Ohnishi, 1998), and the number and location of ubiquinone-binding sites (Okun *et al.*, 1999a). In addition, the chemistry and the sequential formation of possible intermediates in the redox reactions of ubiquinone are expected to play an important role in the reaction mechanism (Brandt, 1997). At present, remarkably few of the parameters defining these constraints are known.

From a conceptual point of view and in analogy to the cytochrome bc_1 complex (Brandt and Trumpower, 1994), one could consider that in complex I proton pumping is linked to the redox-dependent protonation and deprotonation reactions of ubiquinone. Oxidation of ubiquinol is kinetically difficult because the abstraction of the first proton would have to precede electron transfer and this deprotonation reaction has a rather high pK_a value (Brandt, 1997). In the cytochrome bc_1 complex, the oxidation of ubiquinol is promoted by the high midpoint potential of the "Rieske" iron–sulfur cluster, which seems to function as a trap for QH^- (Brandt, 1999a). In complex I, however, the net reaction is the reduction of ubiquinone and the midpoint potentials of the Fe–S clusters involved are rather low. If ubiquinol oxidation should be involved in the catalytic cycle of complex I as a means to release protons on the cytosolic side, there must be some other mechanism to overcome the initial barrier of the reaction.

There are several reasons to propose a key role for cluster N2 in the electron transfer and proton-pumping reactions of complex I (Ohnishi, 1998; Brandt, 1997). The midpoint potential of cluster N2 is pH dependent with a

linear slope of −60 mV/pH unit between −100 mV at pH 6 and −250 mV at pH 8.5 (Ingledew and Ohnishi, 1980). The corresponding pK_a values are not known, but must be above 8.5 for the reduced and below 6 for the oxidized form. This intriguing feature of N2 is typical for a "redox Bohr group" cycling between a base in the reduced state and an acid in the oxidized state, that could be employed as a critical component of a proton pump. It is tempting to speculate that it is reduced cluster N2 which abstracts the first proton from enzyme-bound ubiquinol facilitating its subsequent oxidation by another acceptor (Brandt, 1997). In EPR measurements, using tightly coupled submitochondrial particles, a splitting of the N2 signal was observed, which has been proposed to originate from its paramagnetic coupling with a semiquinone radical (Vinogradov *et al.*, 1995). Based on this assumption, a distance of about 10 Å to the uncoupler-sensitive semiquinone was estimated.

One of the most critical constraints for a complex I mechanism is the number of ubiquinone-binding sites. Inhibitors have proved to be a valuable tool in exploring ubiquinone binding sites in the cytochrome bc_1 complex and in the photoreaction center. In complex I, a large number of chemically rather diverse compounds are known to inhibit reduction of ubiquinone. These inhibitors have been divided into two or three classes depending on their behavior in steady-state kinetics (Degli Esposti, 1998; Friedrich *et al.*, 1994). This classification allowed and promoted hypothetical models involving more than one ubiquinone binding site (Dutton *et al.*, 1998; Degli Esposti and Ghelli, 1994; Brandt, 1997).

In our laboratory, a comprehensive study has been carried out for monitoring the competition between different inhibitors for binding to the enzyme, using the fluorescence quench technique and a radio ligand-binding assay as two independent methods (Okun *et al.*, 1999a,b). The results consistently showed that complex I accommodates inhibitors of all classes in only one extended binding pocket with overlapping binding sites. This finding strongly suggests that in complex I there is only one ubiquinone-binding site that exchanges substrate with the bulk during turnover. This leads to the conclusion that any ubiquinone cycle-type mechanism is highly unlikely for complex I. Together with the close spatial relationship between iron–sulfur cluster N2 and a semiquinone radical (Vinogradov *et al.*, 1995) this seems to imply that the experimentally determined ratio of $2H^+/e^-$ is achieved by a single integrated molecular pump that is assembled in a catalytic core (Kashani-Poor *et al.*, submitted) rather than by two spatially and functionally distinct pumping modules (Friedrich and Scheide, 2000).

Location

Several subunits of complex I exhibit homology to subunits of [NiFe] hydrogenases from various eubacterial and archaebacterial sources. This suggests a common evolutionary origin for these two classes of enzymes (Friedrich and Scheide, 2000). Water soluble [NiFe] hydrogenases consist of two proteins of which the molecular structures have been solved (Volbeda *et al.*, 1995; Montet *et al.*, 1997). The large subunit, which contains the [NiFe] site coordinated by four cysteine ligands, corresponds to the 49 kDa subunit of complex I, while the small subunit, which harbors three iron–sulfur clusters, corresponds to PSST. In membrane bound [NiFe] hydrogenases, a large portion of the small subunit, together with two iron–sulfur clusters is missing. Interestingly, a novel subunit (TYKY in complex I) containing two iron–sulfur clusters in a ferredoxinlike arrangement (Kintscher *et al.*, 2000) was acquired by these enzymes. In complex I, the [NiFe] site has been lost and a novel electron input device, comprising the 75, 51, and 24 kDa subunits was added. Two hydrophobic subunits that serve as membrane anchors of hydrogenases also have homologs in complex I, namely, the mitochondrially encoded subunits ND1, ND4, or ND5. The latter two are related to each other and may have arisen by gene duplication (Finel, 1998).

In recent years, there has been increasing evidence that the subunits conserved between complex I and membrane-bound hydrogenases play a critical role in catalysis. (1) a point mutation resulting in resistance to quinone-related inhibitors was identified in the 49 kDa subunit of complex I from *Rhodobacter capsulatus*, demonstrating a critical role for this subunit in the interaction with ubiquinone (Darrouzet *et al.*, 1998); (2) labeling of bovine complex I with the photoreactive derivative of the inhibitor pyridaben occurred specifically at the PSST subunit, while low-affinity labeling was also found at the ND1 subunit (Schuler *et al.*, 1999); (3) reconstruction of the ND1/3460 mutation, which causes LHON in humans, in a bacterial model system changes the K_m for short-chain ubiquinone analogs. This implies a contribution of ND1 to the ubiquinone-binding site possibly via a surface helix (Zickermann *et al.*, 1998); (4) site-directed mutagenesis of conserved acidic residues in the PSST homolog (Ahlers *et al.*, 2000a) has yielded effects on the EPR signal of cluster N2, the interaction of complex I with the substrate DBQ, and hydrophobic inhibitors and the pH dependence of complex I activity; (5) recently, it has been demonstrated that human Leigh syndrome can be caused by point mutations affecting NDUFS7 (Triepels *et al.*, 1999) and NDUFS8 (Loeffen *et al.*, 1998), the homologs of bovine

PSST and TYKY, respectively. Mutations at corresponding positions were reconstructed in the *Y. lipolytica* system, followed by isolation and *in vitro* characterization of the mutant enzymes (Ahlers *et al.*, 2000b). This study suggested that NDUFS7-V122M and NDUFS8-P97L, the mutations most likely responsible for the disease phenotype (NDUFS8-R102H appears to be more defective and, by this argument, probably recessive), both have similar effects on the enzyme's interaction with the substrate ubiquinone.

Structural Model

The homology of two-subunit water-soluble hydrogenases from several *Desulfovibrio* species (Higuchi *et al.*, 1997; Montet *et al.*, 1997) to the 49 kDa and PSST subunits of complex I has been discussed for many years. It has been established that the 49 kDa subunit contains some highly conserved motifs characteristic for [NiFe] binding subunits in hydrogenases (Albracht, 1993). These motifs were tentatively proposed to be involved in proton translocation in both enzymes.

Recently, we demonstrated that amino acids conserved between the 49 kDa subunit of complex I and the large subunit of [NiFe] hydrogenases are functionally critical and identified structural domains that have been conserved between these enzymes (Kashani-Poor *et al.*, submitted). The first clue in this direction came from the finding that the V470M substitution in the 49 kDa subunit of complex I, detected in an inhibitor-resistant mutant of *Rhodobacter capsulatus* (Darrouzet *et al.*, 1998), lines up with a cysteine ligand of the [NiFe] site in the membrane-bound hydrogenase of *Methanosarcina barkeri* (Meuer *et al.*, 1999) and that this valine (V406 in *Y. lipolytica*) is strictly conserved in complex I. We then found that two of the remaining three [NiFe] cysteine ligands, C72 and C546, were replaced by acidic residues (D143 and E463 in *Y. lipolytica*) in all known 49 kDa subunit sequences. Remarkably, in complex I from *Y. lipolytica*, site-directed mutation of V406, D143, and E463 all led to inhibitor resistance (see below).

With experimental data to back up the hypothesis of a structural conservation between the active sites of hydrogenase and complex I, advantage was taken of the molecular structures available for the large and small subunits of water-soluble hydrogenases (Montet *et al.*, 1997; Volbeda *et al.*, 1995) to obtain insight into the structure of complex I: While the homology between the large and small subunits of *Desulfovibrio* hydrogenases and the corresponding 49 kDa and PSST subunits of complex I is too poor to align the protein sequences reliably, a similarity score of 40% and an identity score of 31% between EchE of *M. barkeri* [NiFe] hydrogenase and the 49 kDa subunit of complex I from *Y. lipolytica* allowed for unambiguous assignment of domains in complex I to corresponding parts of the [NiFe] active site of hydrogenase (Fig. 2A). It is worth noting that the homology between the membrane-bound hydrogenase of *M. barkeri* and complex I is generally better than the homology between water-soluble and the membrane bound hydrogenases.

Assuming that during evolution, structural folds are retained to a much greater extent than sequences, we translated the sequence alignment into a structural comparison (Fig. 2B–D). Four loops make close contact with the [NiFe] site in *D. fructosovorans* hydrogenase. Two of them contribute two of the cysteine ligands (C72/C75 and C543/C546, respectively). The C72/C75 loop is part of a larger domain that comprises the RGXE motif, which is in close contact with the [NiFe] site, two antiparallel helixes connected by a loop, and the loop containing C72 and C75. Of the remaining two loops, one carries a strictly conserved histidine at its tip (H228) and one contains a conserved proline (P475). Three of the cysteine ligands (C72, C543, and C546) correspond to strictly conserved residues in complex I (D143, V460, and E463). Five residues located in the immediate vicinity of the [NiFe] site, namely, R50, G51, E53, R70, and D541 are conserved between all known [NiFe] hydrogenase and all known complex I sequences (R121, G122, E124, R141,

Fig. 2. Model for the catalytic core of complex I based on the structure of the water-soluble [NiFe] hydrogenase from *D. fructosovorans*. (A) Alignment of four loops surrounding the [NiFe] site in the large subunit of water-soluble hydrogenase from *D. fructosovorans* (Montet *et al.*, 1997) with the corresponding sequences in the EchE subunit of membrane-bound [NiFe] hydrogenase from *M. barkeri* (Meuer *et al.*, 1999) and the 49 kDa subunit of complex I from *Y. lipolytica* (Djafarzadeh *et al.*, 2000). Cysteines are marked in yellow, while corresponding conserved acidic residues in complex I are marked in red. Residues conserved between water-soluble hydrogenases and complex I are marked in green. (B) Stereo view of the domains surrounding the [NiFe] site in the water-soluble hydrogenase from *D. fructosovorans*. (C) Position of selected residues in the large subunit of water-soluble hydrogenase from *D. fructosovorans*. (D) Position of residues in the 49 kDa subunit of complex I from *Y. lipolytica* corresponding to the residues in water-soluble hydrogenase from *D. fructosovorans* shown in (C) and the effects on complex I of site-directed mutations in these residues (Kashani-Poor *et al.*, submitted). The structural images were generated from 1FRF coordinates of the PDB-Brookhaven database using the MolMol 2K.1 program on a PentiumIII/NT4.0 workstation.

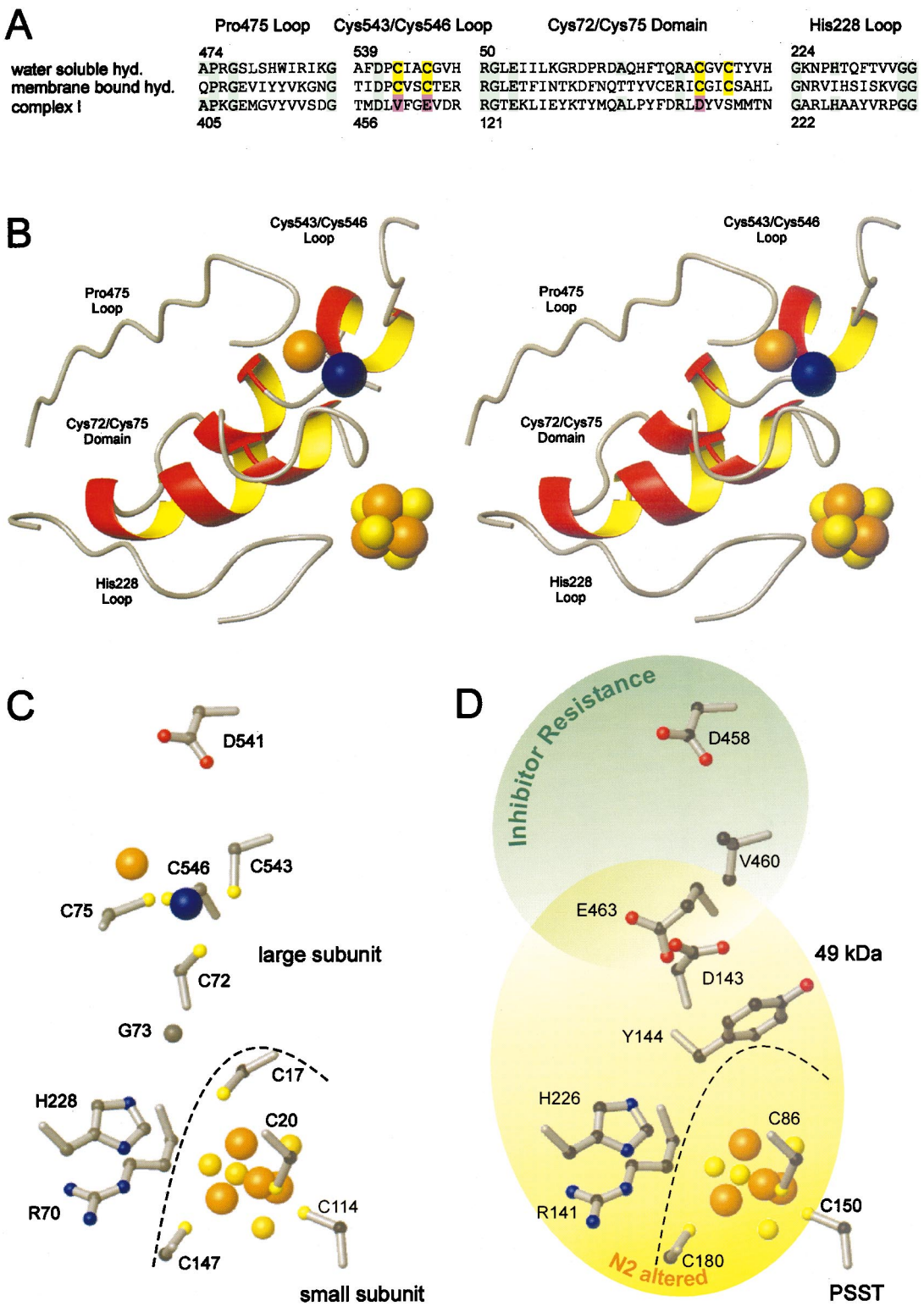
A
Pro475 Loop
Cys543/Cys546 Loop
Cys72/Cys75 Domain
His228 Loop
474
539
50
224
water soluble hyd.
membrane bound hyd.
complex I
APRGSLSHWIRIKG AFDPCIACGVH RGLEIILKGRDPRDAQHFTQRACGVCTYVH GKNPHTQFTVVGG
QPRGEVIYYVKGNG TIDPCVSCTER RGLETFINTKDFNQTTYVCERICGICSAHL GNRVIHSISKVGG
APKGEMGVYVVSDG TMDLVFGEVDR RGTEKLIEYKTYMQALPYFDRLDYVSMMTN GARLHAAYVRPGG
405
456
121
222
B
Cys543/Cys546 Loop
Pro475 Loop
Cys72/Cys75 Domain
His228 Loop
Cys543/Cys546 Loop
Pro475 Loop
Cys72/Cys75 Domain
His228 Loop
C
D541
C546
C543
C75
large subunit
C72
G73
C17
H228
C20
R70
C114
C147
small subunit
D
Inhibitor Resistance
D458
V460
E463
49 kDa
D143
Y144
H226
C86
R141
C150
C180
N2 altered
PSST

and D458). H228 corresponds to a strictly conserved histidine in complex I (H226), but is not found in the homologous membrane-bound hydrogenases. In addition, several glycine residues, *e.g.*, at a critical turn at the base of the H228 loop, are invariantly found in complex I and hydrogenase sequences. This remarkable degree of locally defined sequence conservation further supports the notion that although the metal ion site itself was lost, the structural fold around the [NiFe] active site has been retained and has evolved to become part of the ubiquinone reactive site in complex I.

Most recently, in several complex I-deficient patients, point mutations in NDUFS2 were discovered within the P475 and the H228 loops (Loeffen *et al.*, 2001). These remarkable findings not only emphasize the functional importance of the 49 kDa subunit as such, but highlight two of the domains that we have predicted to be close to the former hydrogenase [NiFe] site.

Site-Directed Mutagenesis

A series of point mutations at crucial positions in the 49 kDa subunit of *Y. lipolytica* complex I support the idea that the catalytic core of complex I has evolved from the [NiFe] active site of hydrogenase (Kashani-Poor *et al.*, submitted). Two different types of mutants could be identified (Fig. 2D): Mutations of residues that line up with the [NiFe] ligating cysteines of hydrogenase (D143, V460, and E463) lead to inhibitor resistance. This holds in particular for the V460M mutation that corresponds to the V407M substitution that had been reported to confer resistance to quinone analogous inhibitors to complex I from *R. capsulatus* (Darrouzet *et al.*, 1998). Mutating the invariant D458 to alanine led to even more pronounced resistance to DQA and rotenone. Considering our proposed structural model, all residues exhibiting inhibitor resistance are predicted to be close to each other and to reside in the domain of the former [NiFe] site. These data suggest that the residues shown in the upper part of the structural model in Fig. 2D contribute to or are in the vicinity of the inhibitor and ubiquinone-binding pocket of complex I.

A second type of mutant characterized in complex I from *Y. lipolytica* did not change inhibitor sensitivity but affected iron–sulfur cluster N2 in a drastic manner. Mutations of invariant residues R141 and H226, identical in water-soluble hydrogenase and complex I, decrease complex I activity and result in an iron–sulfur cluster N2 not detectable by EPR spectroscopy. Exchanging Y144, which in complex I takes the position of an invariant glycine found in hydrogenase, with histidine, alters the EPR line shape of iron–sulfur cluster N2. This is in line with the assumption that R141, H226, and Y144 are close to the ligation sphere of this redox group, as suggested by our comparative structural analysis.

These results provide strong evidence that the residues invariant in the large subunit of [NiFe] hydrogenases and the 49 kDa subunit are of critical importance in complex I. As the effects on N2 become more severe, the closer the mutations come to the position where the proximal iron–sulfur cluster is found in the small subunit of hydrogenase, it seems inevitable to conclude that this cluster has, in fact, become cluster N2 in subunit PSST of complex I.

Structural Implications

Our results demonstrate a remarkable degree of structural conservation between two classes of functionally quite different enzymes on a molecular level. The structural model of the catalytic core of complex I presented here for the first time allows to focus functional studies on specific domains of a small number of subunits in this multisubunit enzyme. Our mutagenesis study demonstrates that the ubiquinone-binding site resides, at least partly, in the 49 kDa subunit and that the subunit bearing iron–sulfur cluster N2 is in close contact with this subunit.

In water-soluble hydrogenases, the [NiFe] active site delivers the electrons from hydrogen oxidation to the proximal iron–sulfur cluster of the small subunit. In complex I, it is generally accepted that the immediate electron donor to ubiquinone is the [4Fe–4S] cluster N2 that has been suggested to be an important component of the proton-translocating machinery (Brandt, 1997). There has been conflicting evidence whether this redox group resides in the TYKY (Chevallet *et al.*, 1997) or in the PSST subunit (Friedrich, 1998). If the latter is true, iron–sulfur cluster N2 would correspond to the proximal iron–sulfur cluster of hydrogenase. This would position it ideally to donate electrons to ubiquinone in a catalytic site that has evolved from the hydrogen reactive [NiFe] site of hydrogenase. However, in this case, one of the four ligands of the proximal iron–sulfur cluster (C75, Fig. 2C) not present in the PSST subunit must have been replaced by another residue. Based on structural homology and the results from our site-directed mutagenesis study, one is tempted to speculate that the fourth ligand of N2 actually resides on the 49 kDa subunit. Possible candidates are the invariant H226 that already in hydrogenase makes a hydrogen bond to the proximal iron–sulfur cluster (Volbeda *et al.*, 1995) and the fully conserved Y144 that has replaced the conserved G73 of hydrogenase (cf. Fig. 2C, D).

We propose that the terminal segment of the electron transfer chain leading to the ubiquinone-reactive site is formed by the two EPR-silent [4Fe–4S] clusters N6a and

N6b in the ferredoxinlike subunit TYKY (Yano *et al.*, 1999; Kintscher *et al.*, 2000) and the nonconventional [4Fe–4S] cluster N2 residing in subunit PSST (Friedrich, 1998). The missing fourth ligand could not be found in subunit PSST (Ahlers *et al.*, 2000a) and we suggest that it may reside in the adjacent domains of the 49 kDa subunit of complex I. This part of the 49 kDa subunit contains critical parts of the catalytic core of complex I. Other contributions may come from adjacent parts of subunit PSST and peripheral domains of the hydrophobic subunits ND1, ND4, and/or ND5. This hypothesis would be in line with the finding of inhibitor-resistant mutants in the 49 kDa subunit, the pyridaben-labeling of the PSST subunit (Schuler *et al.*, 1999), and the labeling of subunit ND1 by a rotenone-derived photoaffinity label (Earley *et al.*, 1987).

Functional Implications

At this stage, any proposal of a complex I mechanism still has to be highly speculative. However, compilation of all available information provides some useful mechanistic constraints.

While FMN and the other iron–sulfur clusters function in electron uptake and conversion of the two electron input into one electron transfer steps, N2 with its associated redox Bohr group seems to play a key role in proton translocation across the membrane. Based on the experimental pump stoichiometry of 2 H^+/e^-, two coupling sites in complex I were postulated (Friedrich *et al.*, 1998), one of them being a yet undefined, but spectroscopically characterize, group X (Schulte *et al.*, 1999).

However, our structural model derived from [NiFe] hydrogenases rather suggests that the coupling of electron flow and proton pumping is confined to a catalytic core forming a spatially and functionally integrated pump. The semiquinone switch mechanism (Brandt, 1999b), which could operate in such a device accounts for the observed pump stoichiometry. It employs three different elements: (1) a single substrate binding site; (2) a tightly bound quinone or quinoid group X; and (3) iron–sulfur cluster N2. Upon reduction of N2, the pK_a value of the associated redox Bohr group increases and a proton is abstracted from the tightly bound ubiquinol or reduced quinoid group, allowing its subsequent oxidation by the substrate ubiquinone to the semiquinone state. The proton on N2 is ejected to the positive side of the membrane upon reoxidation of N2 by the prosthetic semiquinone. Repeating this reaction sequence results in net reduction of one substrate ubiquinone and in a translocation of $4H^+/2e^-$ if cycling between the prosthetic semiquinone is linked to proton uptake from the matrix side and proton release—potentially via N2—to the cytosolic side.

REFERENCES

Ahlers, P., Zwicker, K., Kerscher, S., and Brandt, U. (2000a). *J. Biol. Chem.* **275**, 23577–23582.

Ahlers, P., Garofano, A., Kerscher, S., and Brandt, U. (2000b). *Biochim. Biophys. Acta* **1459**, 258–265.

Albracht, S. P. J. (1993). *Biochim. Biophys. Acta* **1144**, 221–224.

Barth, G., and Gaillardin, C. (1996). In *Non-Conventional Yeasts in Biotechnology* (K. Wolf, ed.), Springer, Berlin-Heidelberg, pp. 313–388.

Barth, G., and Gaillardin, C. (1997). *FEMS Microbiol. Rev.* **19**, 219–237.

Brandt, U. (1997). *Biochim. Biophys. Acta* **1318**, 79–91.

Brandt, U. (1999a). *J. Bioenerg. Biomembr.* **31**, 243–250.

Brandt, U. (1999b). *BioFactors* **9**, 95–101.

Brandt, U., and Trumpower, B. L. (1994). *CRC Crit. Rev. Biochem.* **29**, 165–197.

Chevallet, M., Dupuis, A., Lunardi, J., van Belzen, R., Albracht, S. P. J., and Issartel, J. P. (1997). *Eur. J. Biochem.* **250**, 451–458.

Darrouzet, E., Issartel, J. P., Lunardi, J., and Dupuis, A. (1998). *FEBS Lett.* **431**, 34–38.

Degli Esposti, M. (1998). *Biochim. Biophys. Acta* **1364**, 222–235.

Degli Esposti, M., and Ghelli, A. X. (1994). *Biochim. Biophys. Acta* **1187**, 116–120.

Djafarzadeh, R., Kerscher, S., Zwicker, K., Radermacher, M., Lindahl, M., Schägger, H., and Brandt, U. (2000). *Biochim. Biophys. Acta* **1459**, 230–238.

Dutton, P. L., Moser, C. C., Sled, V. D., Daldal, F., and Ohnishi, T. (1998). *Biochim. Biophys. Acta* **1364**, 245–257.

Earley, F. G., Patel, S. D., Ragan, C. I., and Attardi, G. (1987). *FEBS Lett.* **219**, 108–112.

Finel, M. (1998). *Biochim. Biophys. Acta* **1364**, 112–121.

Friedrich, T. (1998). *Biochim. Biophys. Acta* **1364**, 134–146.

Friedrich, T., and Scheide, D. (2000). *FEBS Lett.* **479**, 1–5.

Friedrich, T., van Heek, P., Leif, H., Ohnishi, T., Forche, E., Kunze, B., Jansen, R., Trowitzsch-Kienast, W., Höfle, G., Reichenbach, H. X., and Weiss, H. (1994). *Eur. J. Biochem.* **219**, 691–698.

Friedrich, T., Abelmann, A., Brors, B., Guenebaut, V., Kintscher, L., Leonard, K., Rasmussen, T., Scheide, D., Schlitt, A., Schulte, U., and Weiss, H. (1998). *Biochim. Biophys. Acta* **1365**, 215–219.

Grigorieff, N. (1998). *J. Mol. Biol.* **277**, 1033–1046.

Herter, S. M., Schiltz, E., and Drews, G. (1997). *Eur. J. Biochem.* **246**, 800–808.

Higuchi, Y., Yagi, T., and Yasuoka, N. (1997). *Structure* **5**, 1671–1680.

Ingledew, W. J., and Ohnishi, T. (1980). *Biochem. J.* **186**, 111–117.

Kashani-Poor, N., Kerscher, S., Zickermann, V., and Brandt, U. (2001). *Biochim. Biophys. Acta* **1504**, 363–370.

Kashani-Poor, N. *et al.*, submitted.

Kerscher, S., Okun, J. G., and Brandt, U. (1999). *J. Cell Sci.* **112**, 2347–2354.

Kerscher, S., Durstewitz, G., Casaregola, S, Gaillardin, C., and Brandt, U. (2001). *Comparative and Functional Genomics*, in press.

Kerscher, S. *et al.*, submitted.

Kintscher, L., Rasmussen, T., Scheide, D., Weiss, H., and Friedrich, T. (2000). *EBEC Short Rep.* **11**.

Kowal, A. T., Morningstar, J. E., Johnson, M. K., Ramsay, R. R., and Singer, T. P. (1986). *J. Biol. Chem.* **261**, 9239–9245.

Krebs, W., Steuber, J., Gemperli, A. C., and Dimroth, P. (1999). *Mol. Microbiol.* **33**, 590–598.

Leif, H., Sled, V. D., Ohnishi, T., Weiss, H., and Friedrich, T. (1995). *Eur. J. Biochem.* **230**, 538–548.

Loeffen, J., Smeitink, J., Triepels, R., Smeets, R., Schuelke, M., Sengers, R., Trijbels, F., Hamel, B., Mullaart, R., and Van den Heuvel, L. (1998). *Amer. J. Human. Genet.* **63**, 1598–1608.

Loeffen, J., Elpeleg, O., Smeitink, J., Smeets, R., Stöckler-Ipsiroglu, S., Mandel, R., Sengers, R., Trijbels, F., and Van den Heuvel, L. (2001). *Ann. Neurol.* **49**, 195–201.

Luttik, M. A. H., Overkamp, K. M., Kötter, P., de Vries, S., van Dijken, P., and Pronk, J. T. (1998). *J. Biol. Chem.* **273**, 24529–24534.

Madzak, C., Blanchin-Roland, S., Otero, R. C., and Gaillardin, C. (1999). *Microbiology* **145**, 75–87.

Madzak, C., Treton, B., and Blanchin-Roland, S. (2000). *J. Mol. Microbiol. Biotechnol.* **2**, 207–216.

Meuer, J., Bartoschek, S., Koch, J., Künkel, A., and Hedderich, R. (1999). *Eur. J. Biochem.* **265**, 325–335.

Montet, Y., Amara, P., Volbeda, A., Vernede, X., Hatchikian, E. C., Field, M. J., Frey, M., and Fontecilla-Camps, J. C. (1997). *Nat. Struct. Biol.* **4**, 523–526.

Ohnishi, T. (1998). *Biochim. Biophys. Acta* **1364**, 186–206.

Ohnishi, T., Blum, H., Galante, Y. M., and Hatefi, Y. (1981). *J. Biol. Chem.* **256**, 9216–9220.

Okun, J. G., Lümmen, P., and Brandt, U. (1999a). *J. Biol. Chem.* **274**, 2625–2630.

Okun, J. G., Zickermann, V., and Brandt, U. (1999b). *Biochem. Soc. Trans.* **27**, 596–601.

Radermacher, H. *et al.*, in preparation.

Robinson, B. H. (1998). *Biochim. Biophys. Acta* **1364**, 271–286.

Schapira, A. H. (1998). *Biochim. Biophys. Acta* **1364**, 261–270.

Schon, E. A. (2000). *Trends Biochem. Sci.* **25**, 555–560.

Schuler, F., Yano, T., Di Bernardo, S., Yagi, T., Yankovskaya, V., Singer, T. P., and Casida, J. E. (1999). *Proc. Natl. Acad. Sci. USA* **96**, 4149–4153.

Schulte, U., Haupt, V., Abelmann, A., Fecke, W., Brors, B., Rasmussen, T., Friedrich, T., and Weiss, H. (1999). *J. Mol. Biol.* **292**, 569–580.

Skehel, J. M., Fearnley, I. M., and Walker, J. E. (1998). *FEBS Lett.* **438**, 301–305.

Sled, V. D., Friedrich, T., Leif, H., Weiss, H., Fukumori, Y., Calhoun, M. W., Gennis, R. B., Ohnishi, T., and Meinhardt, S. W. (1993). *J. Bioenerg. Biomembr.* **25**, 347–356.

Smeitink, J., and Van den Heuvel, L. (1999). *Amer. J. Human Genet.* **64**, 1505–1510.

Spehr, V., Schlitt, A., Scheide, D., Guénebaut, V., and Friedrich, T. (1999). *Biochemistry* **38**, 16261–16267.

Steuber, J., Schmid, C., Rufibach, M., and Dimroth, P. (2000). *Mol. Microbiol.* **35**, 428–434.

Triepels, R., Van den Heuvel, L. P., Loeffen, J. L., Buskens, C. A., Smeers, R. J. P., Rubio-Gozalbo, M. E., Budde, S. M. S., Mariman, E. C. M., Wijburg, F. A., Barth, P. G., Trijbels, J. M., and Smeitink, J. A. (1999). *Ann. Neurol.* **45**, 787–790.

Vinogradov, A. D., Sled, V. D., Burbaev, D. S., Grivennikova, V. G. X., Moroz, I. A., and Ohnishi, T. (1995). *FEBS Lett.* **370**, 83–87.

Volbeda, A., Charon, M. H., Piras, C., Hatchikian, E. C., Frey, M., and Fontecilla-Camps, J. C. (1995). *Nature (London)* **373**, 580–587.

Walker, J. E. (1992). *Quart. Rev. Biophys.* **25**, 253–324.

Wallace, D. C. (1994). *Proc. Natl. Acad. Sci. USA* **91**, 8739–8746.

Wallace, D. C. (1999). *Science* **283**, 1482–1488.

Wang, D.-C., Meinhardt, S. W., Sackmann, U., Weiss, H., and Ohnishi, T. (1991). *Eur. J. Biochem.* **197**, 257–264.

Wikström, M. K. F. (1984). *Nature (London)* **308**, 558–560.

Yagi, T., Yano, T., Di Bernardo, S., and Matsuno-Yagi, A. (1998). *Biochim. Biophys. Acta* **1364**, 125–133.

Yano, T., Magnitsky, S., Sled, V. D., Ohnishi, T., and Yagi, T. (1999). *J. Biol. Chem.* **274**, 28598–28605.

Zickermann, V., Barquera, B., Wikström, M. K. F., and Finel, M. (1998). *Biochemistry* **37**, 11792–11796.